ACS SyntheticBiology

Research Article

pubs.acs.org/synthbio

A Synthetic Post-transcriptional Controller To Explore the Modular Design of Gene Circuits

Francesca Ceroni,*[,†,+] Simone Furini,[‡,+] Alessandra Stefan,[§,∥] Alejandro Hochkoeppler,[§,∥] and Emanuele Giordano[†,⊥]

[†]Laboratory of Cellular and Molecular Engineering, University of Bologna, I-47521 Cesena, Italy

[‡]Department of Medical Surgery and Bioengineering, University of Siena, I-53100 Siena, Italy

[§]Department of Industrial Chemistry, University of Bologna, Viale Risorgimento 4, I-40136 Bologna, Italy

[∥]CSGI, University of Firenze, Via della Lastruccia 3, I-50019 Sesto Fiorentino, Italy

[⊥]Department of Biochemistry "G. Moruzzi", University of Bologna, I-40126 Bologna, Italy

Supporting Information

ABSTRACT: The assembly from modular parts is an efficient approach for creating new devices in Synthetic Biology. In the "bottom-up" designing strategy, modular parts are characterized in advance, and then mathematical modeling is used to predict the outcome of the final device. A prerequisite for bottom-up design is that the biological parts behave in a modular way when assembled together. We designed a new synthetic device for post-transcriptional regulation of gene expression and tested if the outcome of the device could be described from the features of its components. Modular parts showed unpredictable behavior when assembled in different complex circuits. This prevented a modular description of the device that was possible only under specific conditions. Our findings shed doubts into the feasibility of a pure bottom-up approach in synthetic biology, highlighting the urgency for new strategies for the rational design of synthetic devices.

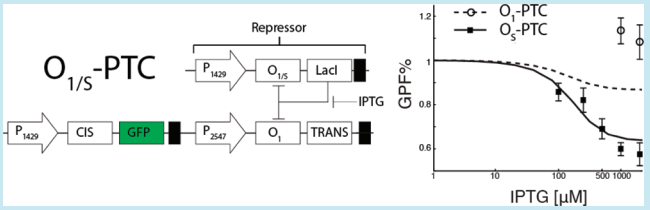

KEYWORDS: *bottom-up approach, post-transcriptional regulation, synthetic biology*

Synthetic biology aims at the rational design of gene networks guided by *a priori* analysis of the features of their basic components.[1,2] We previously developed a synthetic device for the transcriptional control of gene expression, using modular parts and a "bottom-up" approach.[3] Only when the modular parts were characterized in the appropriate environment, i.e., a gene network similar to the final device, was a quantitative prediction of the response of the gene network possible. Thus, for bottom-up design to become a practical strategy in synthetic biology, it is necessary to establish to what extent the elementary components of the network behave as independent modules when moved from one network to another. We here present a synthetic post-transcriptional controller of gene expression intended as a tool to investigate if the outcome of this network can be predicted from the features of its elementary components.

Different devices have been developed so far for the control of gene expression at the transcriptional[4−9] or post-transcriptional[10−12] level. Post-transcriptional regulation allows a faster regulation of gene expression, which might result relevant in the design of synthetic gene circuits.[13,14] In 2004, Isaacs et al.[13] presented a post-transcriptional gene regulation system where two non-coding mRNA sequences were combined to regulate gene expression. Starting from their work, we developed a modular and flexible device for the post-transcriptional regulation of gene expression intended for testing the *modular* approach to the design of gene devices from a collection of known basic components, and as a synthetic tool for the characterization of new elementary parts. To this aim, two new parts were designed and assembled: a CIS-acting and a TRANS-acting non-coding sequence. The CIS element contains a non-coding region and a ribosome binding site (RBS), to be inserted upstream of a gene of interest whose expression will result modulated, e.g., a reporter gene. The TRANS element is complementary to the CIS non-coding region and overlaps on 4 base pairs of the RBS, leading to inhibition of translation. The features of these parts allow the silencing of the gene downstream of the CIS element, independently of the gene sequence itself. Thus, our device can be described as synthetic post-transcriptional controller of the expression of any gene of interest. The silencing mechanism is based on a molecule-to-molecule (TRANS-to-CIS) direct interaction that inhibits translation, leading to an ON-to-OFF switch of gene expression. An OFF-to-ON switch, such as the one described in ref 13, would be easier to be detected in the case of a long degradation time of the reporter gene. However, as GFP degradation in *E. coli* is shorter than one life cycle when degradation tags are used[3,4] and since an ON-to-OFF switch allows a simpler network, this topology was preferred. The

Received: November 14, 2011
Published: April 28, 2012

TRANS sequence was placed under the regulation of the Lac repressor. Thus, the amount of interfering molecules in the cell can be tuned adding the required concentration of the inducer IPTG. The modular topology of our network allows the replacement of the components, e.g., operator sites and promoters, to tune at will the behavior of the system and the resulting gene expression. Each modular component was characterized in gene networks different from the final device. Mathematical modeling was used to simulate the behavior of the complete gene network. The modularity of the synthetic device was tested by comparing model results and experimental data.

RESULTS AND DISCUSSION

In this paper a synthetic molecular device for post-transcriptional regulation of gene expression was developed, and the outcome of the network was analyzed in light of the features of its elementary modules. The goal was to explore to what extent modular parts conserve their functional properties when assembled together, which is a critical property in order to design biomolecular devices using a bottom-up approach. The Registry of Standard Biological parts collects biological components, standardized for a physical modularity. In order to use these parts for the construction of gene devices in living cells, a quantitative characterization of their behavior is needed.[15,16] So far, the standardization introduced by the Registry has greatly improved the physical assembly of parts and devices. However, prediction of the behavior of a gene network out of the properties of its elementary components is feasible only if biological parts, together with a physical modularity, also display a functional modularity.

Definition of the Gene Circuits. *E. coli* CSH126 cells were transformed with two different plasmids, here named *Repressor* and *PT-controller* (Figure 1). The *PT-Controller* plasmid contains two separate modules, referred to as *Reporter* and *Silencer*. The *Reporter* harbors the CIS sequence upstream of a GFP-coding sequence; the *Silencer* codes for the TRANS sequence, complementary to the CIS (see Table 1 for CIS/TRANS sequences). GFP synthesis from the *PT-Controller* depends on the silencing process deriving from TRANS binding to the CIS sequence and overlapping the initial 4 bases of the RBS, thus impeding translation (Figure 1A). The gene circuit encoded in the *Repressor* plasmid has a negative feedback structure as an operator site for LacI inserted downstream of a promoter sequence that controls the expression of the lactose repressor gene itself. The concentration of LacI in the cytoplasm also controls transcription from the *Silencer* by binding to an operator site for LacI placed upstream of the TRANS sequence (Figure 1B). The synthesis of TRANS in cells transformed with both the *Repressor* and the *PT-Controller* plasmids can be tuned using appropriate concentrations of the gratuitous inducer IPTG. Two versions of the *Repressor* plasmid were used, respectively with the O_1 and the O_S operator sequence (see Methods for the O_1 and O_S sequences). Cell-transformed with the *PT-controller* and the *Repressor* with either O_1 or O_S operator sequences are here referred to as O_1-PTC and O_S-PTC, respectively. In order to characterize the modular parts that compose the $O_{1/S}$-PTC gene circuits, alternative circuits including only a subset of the modular elements were also produced.

Silencing of Protein Expression by TRANS−CIS Annealing. Cells transformed with the *Reporter* alone yielded a fluorescence level equal to 9677 ± 2361 and 10307 ± 1561 arbitrary units (au), respectively, in either the presence or absence of the CIS sequence (Figure 2, a,b. The gene circuits corresponding to the labels of Figure 2 are shown in Figure 3). When cells were transformed with the *PT-Controller* lacking the TRANS element, with or without the *Repressor* with the O_1 operator, fluorescence levels were 9974 ± 1154 au and 9867 ± 1314 au, respectively (Figure 2, c,d). In all of the gene circuits described so far, GFP is constitutively expressed under the control of the same promoter, and no additional control on transcription or translation is exerted. The equivalent fluorescent output observed from the cells transformed with these 4 gene circuits (Figure 2, a−d) supports the hypothesis that our gene networks behave as modular. When cells were transformed with the complete *PT-Controller* device, fluorescence decreased to 776 ± 387 au (Figure 2, e), showing that GFP production is repressed in presence of the TRANS sequence. Since in the absence of the TRANS sequence the fluorescence is equal to the maximum value observed in cells transformed with the *Reporter* alone, only the CIS−TRANS annealing interaction accounts for repression of GFP protein expression. Fluorescence levels from cells transformed with the *PT-Controller* lacking the TRANS sequence were chosen as the maximum fluorescence level of the gene circuit. The relative fluorescence (GFP %) observed using various gene circuits and IPTG concentrations is reported as the percentage with respect to this value. The data presented in the manuscript refer to cell samples with OD = 0.9, when not otherwise specified. Significant statistical differences among gene circuits are conserved for small variations of OD around this value (Figure 4).

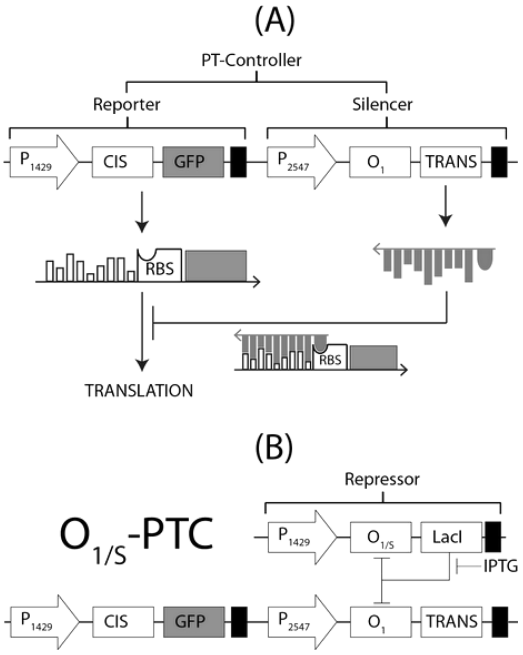

Figure 1. Gene circuits. (A) Gene circuit in cells transformed with *PT-Controller* alone. The TRANS sequence can bind to the CIS, overlapping also to 4 base pairs of the RBS. The CIS−TRANS annealing leads to translation inhibition. (B) Gene circuit in cells transformed with $O_{1/S}$- PTC. LacI from the *Repressor* inhibits TRANS production by binding to the Lac operator O_1, thus increasing GFP translation. The inducer IPTG can be used to tune the amount of interfering molecules inside the cell.

Tuning of Post-transcriptional Control by IPTG. In absence of IPTG, cells transformed with O_1-PTC and O_S-PTC

dx.doi.org/10.1021/sb200021s | *ACS Synth. Biol.* 2012, 1, 163−171

Table 1. CIS and TRANS Sequences[a]

	CIS acting element
non-coding sequence	5′-AACACAAACTATCACTTTAACAACACATTACATATACATTAAAATATTAC-3′
ribosome binding site	5′-AAAGAGGAGAAA-3′
	TRANS acting element
non-coding annealing sequence	3′-TTGTGTTTGATAGTGAAATTGTTGTGTAATGTATATGTAATTTTATAATG-5′
4 base pair RBS cover	3′-TTTC-5′

[a]The CIS element (first section) is a 50-bp-long sequence composed of a non-coding sequence and a ribosome binding site from the Registry of Standard Biological Parts (BBa_B0034). The TRANS element (second section) contains a non-coding region complementary to the CIS non-coding region and 4-bp-long sequence complementary to the first 4 bases of the RBS.

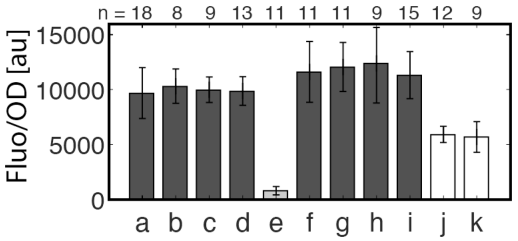

Figure 2. Normalized fluorescence in $O_{1/S}$-PTC and control gene circuits. The labels along the lower *x*-axis identify cells that are transformed with (a) *Reporter* without CIS sequence; (b) *Reporter*; (c) *PT-Controller* without TRANS sequence; (d) *PT-Controller* without TRANS sequence plus *Repressor* with O_1 operator; (e) *PT-Controller*; (f) O_1-PTC; (g) O_1-PTC with 1 mM IPTG; (h) O_1-PTC with 2 mM IPTG; (i) O_s-PTC; (j) O_s-PTC with 1 mM IPTG; (k) O_s-PTC with 2 mM IPTG. The gene circuits corresponding to the labels along the *x*-axis are shown in Figure 3. Values are shown as average ± SD. The number of samples (*n*) is reported along the upper *x*-axis. Cell types belonging to the same group, as determined by the Bonferroni test, have bars of the same colors, while different colors identify cell types that are statistically different.

showed fluorescence of 11598 ± 2768 au and 11308 ± 2152 au (Figure 2, f,i). These fluorescence values are equal to the maximum fluorescence measured in the absence of the TRANS sequence (Figure 2, d), which proves that in these conditions the amount of TRANS sequences in the cells is too low to promote a decrease in GFP translation by the CIS−TRANS annealing reaction. In presence of IPTG, when LacI-induced repression is reduced, one would expect an increase in the amount of TRANS sequences transcribed, with a following decrease in GFP translation. However, when 1 mM IPTG was added to cells transformed with the O_1-PTC gene circuit, fluorescence value was equal to 12060 ± 2238 au (Figure 2, g). Doubling IPTG concentration to 2 mM did not decrease this value (12370 ± 3600; Figure 2, h). These data suggest that the increase in TRANS transcription, induced by IPTG in the O_1-PTC circuit, is not sufficient to inhibit GFP translation by CIS−TRANS annealing. As the use of a stronger operator sequence in the *Repressor* circuit is expected to decrease the amount of available LacI, rendering more effective induction by IPTG, cells were transformed with the O_S-PTC gene circuit. The O_S operator has a higher binding affinity for the lactose repressor,[3,17] and thus these cells were expected to express less LacI molecules than cells transformed with O_1-PTC circuit. Indeed, cells transformed with the O_S-PTC circuit yielded fluorescence values equal to 5908 ± 727 and 5679 ± 1398 au (Figure 2, j,k), after addition of 1 and 2 mM IPTG, respectively. As expected, a stronger operator site in the *Repressor* circuit allowed restoring, at least partially, the TRANS repressing action on GFP translation.

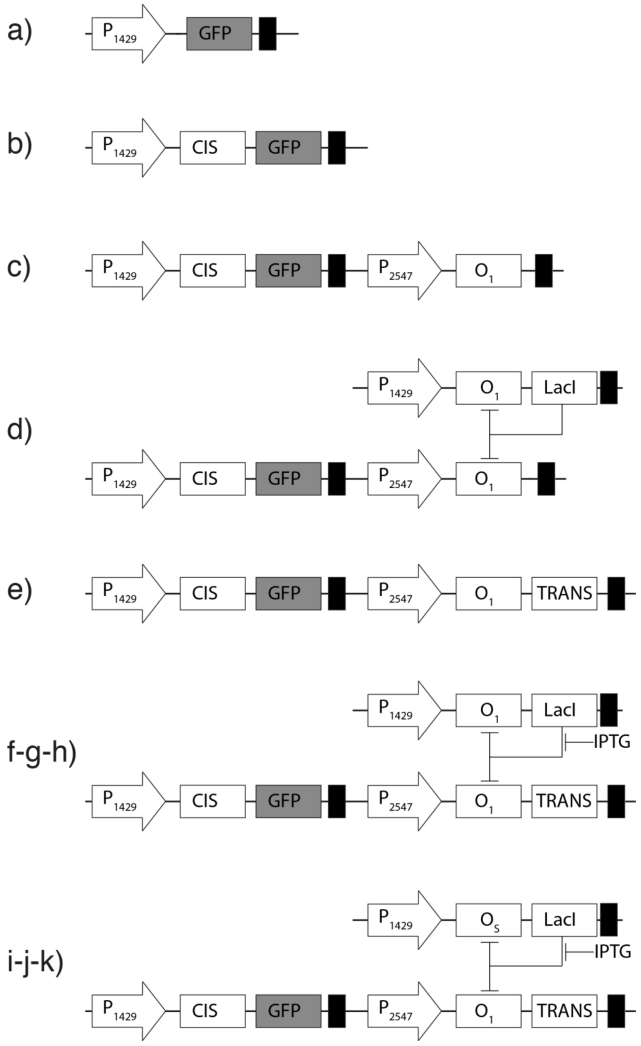

Figure 3. Schematic representation of the gene circuits corresponding to the labels in Figure 2.

Test of the Modularity of the Parts. The $O_{1/S}$-PTC gene circuit is made of two modules, logically separated: (1) the *Repressor* and the *Silencer*, which operate as a source of TRANS sequence controlled by IPTG, and (2) The *Reporter*, which produces GFP molecules, in a TRANS-controlled fashion. In order to characterize the first module, cells were transformed with the gene circuits $O_{1/S}O_1$ and O_1. Circuits $O_{1/S}O_1$ are composed of *Repressor* with either the O_1 or the O_S operator site, respectively, and a different version of the *Silencer* where the TRANS replaces the GFP sequence (Figure 5A). Circuit O_1 included only the *Silencer* modified with the GFP sequence (Figure 5C). GFP expression in cells transformed with the

dx.doi.org/10.1021/sb200021s | ACS Synth. Biol. 2012, 1, 163−171

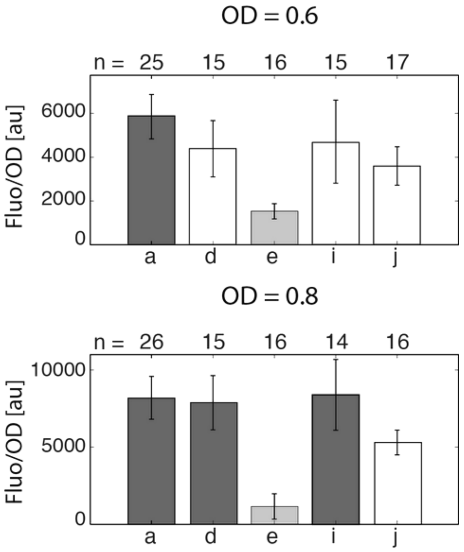

Figure 4. Normalized fluorescence in $O_{1/S}$-PTC and control gene circuits at two different OD values. The labels along the lower *x*-axis identify cells that are transformed with (a) *Reporter* without CIS sequence; (d) *PT-Controller* without TRANS sequence plus *Repressor* with O1 operator; (e) *PT-Controller*; (i) Os-PTC; (j) Os-PTC with 1 mM IPTG. Values are shown as average ± SD. The number of samples (*n*) is reported along the upper *x*-axis. Cell types belonging to the same group, as determined by the Bonferroni test, have bars of the same colors, while different colors identify cell types that are statistically different.

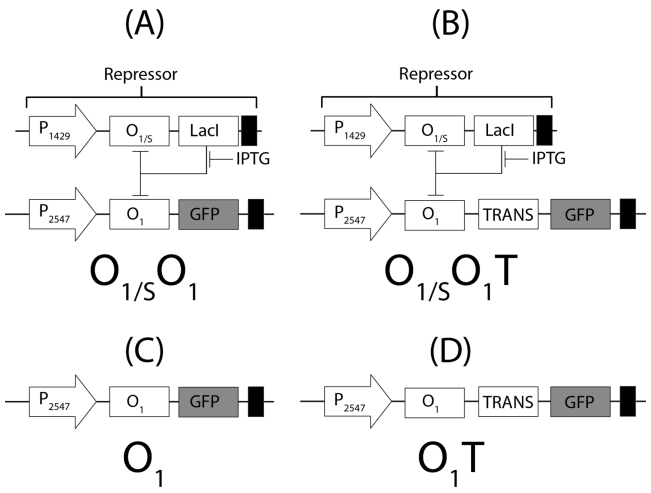

Figure 5. Gene circuits for the *Repressor-Silencer* module. (A) $O_{1/S}O_1$. The *Silencer*, with the TRANS sequence replaced by a GFP protein, is co-transformed with *Repressors* with the O_1 or the O_S operator sites. (B) $O_{1/S}O_1T$. The *Silencer*, with the TRANS sequence placed upstream of the GFP protein, is co-transformed with *Repressors* with the O_1 or the O_S operator sites. (C) O_1. *Silencer* with the TRANS sequence replaced by a GFP protein. (D) O_1T. *Silencer* with the TRANS sequence placed upstream of the GFP sequence.

$O_{1/S}O_1$ gene circuits was sensible to IPTG concentration, with maximum induction at saturating IPTG concentration equal to ∼60% and ∼40% of the fluorescence level in cells transformed with the O_1 circuit, respectively in O_SO_1 and O_1O_1 (Figures 6A and 7). On the basis of these results, in a modular framework, one should expect that at maximum IPTG induction also the synthesis of TRANS would approach ∼60% and ∼40% of the maximum value, respectively, in O_S-PTC and O_1-PTC. A synthesis of TRANS equal to ∼60% and ∼40% of the maximum value should evoke a consistent reduction of fluorescence in the $O_{1/S}$-PTC cells, which we did not observe in our experiments (Figure 2).

A model of the $O_{1/S}$-PTC circuit was defined, and its parameters were determined by experimental measurements on the logical modules 1 and 2 defined in the previous paragraph, in a pure bottom-up approach. Briefly, parameters for the *Repressor* and the *Silencer* were taken by experimental measurements of the $O_{1/S}O_1$ gene circuits, and the decrease in fluorescence in cells transformed with the *PT-Controller* alone was used to define CIS−TRANS affinity (for more details see the Methods section). The predictions of the models widely disagree with the observed experimental results (Figure 6C).

In order to understand the molecular interactions responsible for the deviation from the modular behavior, we analyzed the effect of the TRANS sequence on the gene circuits $O_{1/S}O_1$. An alternative set of circuits was defined, named $O_{1/S}O_1T$ and O_1T, where a TRANS sequence was placed upstream the GFP sequence in the *Silencer* circuit (Figure 5B and D). Fluorescence of cells transformed with the *Silencer* circuit alone, either with (O_1T) or without (O_1) the TRANS sequence, was compared. Unexpectedly, the presence of the TRANS sequence in proximity of the GFP coding sequence enhanced protein expression (Figure 7). This increase in protein expression may be explained by the observation that different sequences at the 5′-UTR can affect transcriptional and translational efficiency.[18−20]

Moreover, the presence of the TRANS sequence also affected IPTG induction. Indeed, when induced by IPTG, cells transformed with the $O_{1/S}O_1T$ gene circuits reached a maximum fluorescence of only ∼30% and ∼10% of the control value, respectively (Figure 6B), compared to ∼60% and ∼40% observed in cells transformed with the $O_{1/S}O_1$ gene circuits. Dose−response curves of the $O_{1/S}O_1T$ gene circuits could be reproduced by the mathematical model developed for the $O_{1/S}O_1$ gene circuits, increasing the affinity of the operator O_1 on the *Silencer* circuit (see Methods for details about the fitting procedure). When a 5-fold increase in affinity was introduced in the mathematical model of the $O_{1/S}$-PTC gene circuits, with no other adjustment in the parameters of the model, the predictions of the model were in agreement with the experimental data (Figure 6D). The agreement between simulated and experimental data is extremely good for O_S-PTC, while in the case of the O_1-PTC the model predicts a reduction of fluorescence to ∼90% of the maximum value, which is not observed in the experimental data. The difference between the predicted dose−response curve and the experimental data might be justified by poor sensibility of the experimental setup, which was inadequate to detect such a low decrease in fluorescence. Note that although in Figure 6 the fluorescence of the cells transformed with O_1-PTC in presence of 1 and 2 mM IPTG appears to be higher than the value of gene circuits without the TRANS sequence (normalization value), these fluorescence values are statistically equal to the normalization value (Figure 2).

A possible explanation for the change in sensitivity to IPTG is that the affinity for the operator sites can be modulated by the sequences of the flanking regions. The idea that flanking regions could affect the behavior of a closed sequence is not new.[21,22] Here, the extent of the change in affinity may be unexpected. In order to reproduce the dose−response curves of the $O_{1/S}O_1T$ gene circuits, the binding affinities of LacI to its

dx.doi.org/10.1021/sb200021s | *ACS Synth. Biol.* 2012, 1, 163−171

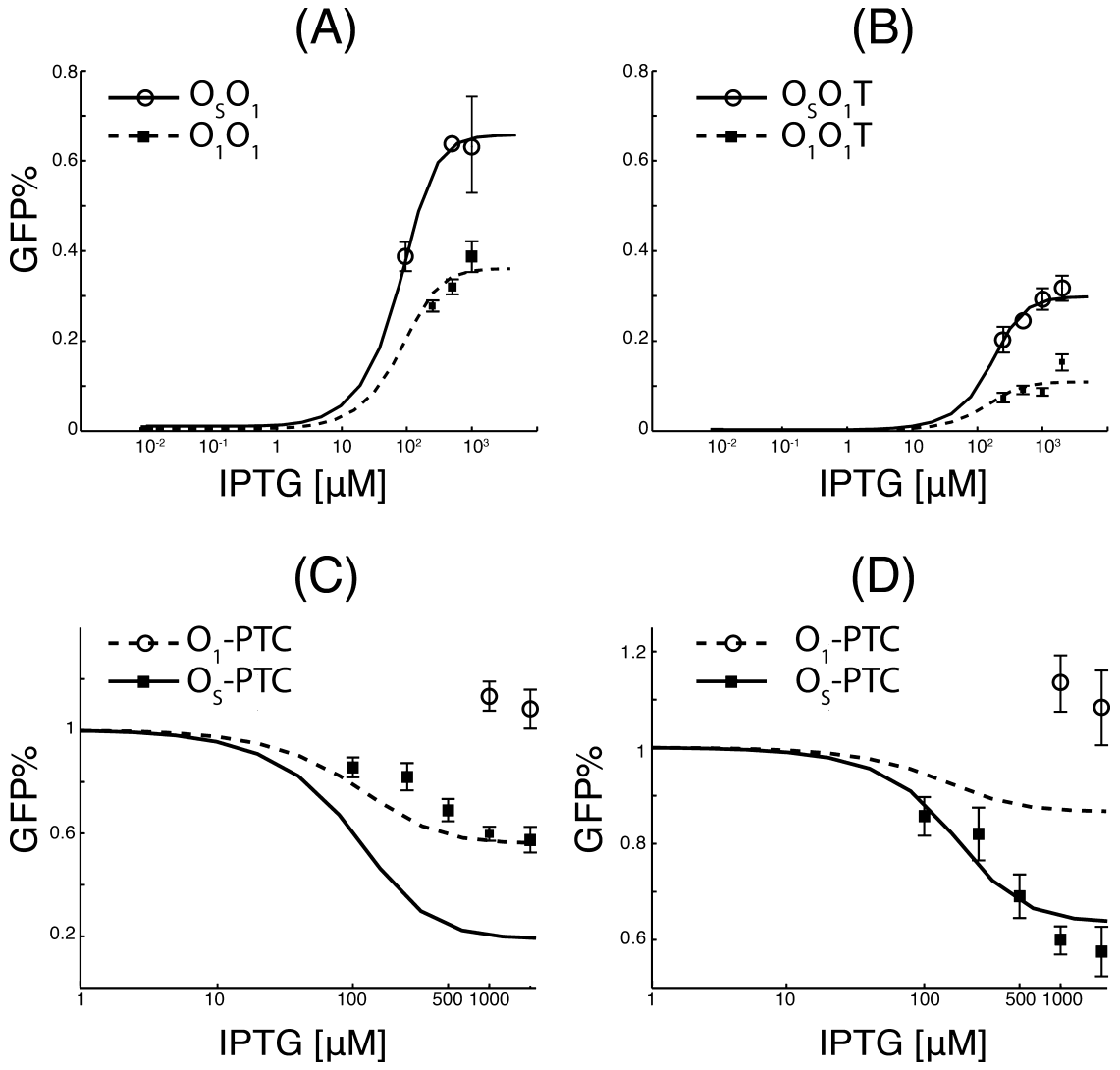

Figure 6. Dose–response curves. Cells were induced with different IPTG concentrations. Experimental data are shown as average values ± SE. The number of samples is above 5 for all of the data shown. Simulated data are shown as continuous and dashed lines, while experimental data are shown as black squares and dots. (A) Induction of the gene circuits O_1O_1 and O_SO_1. (B) Induction of the gene circuits O_1O_1T and O_SO_1T. (C) Induction of the gene circuits O_1-PTC and O_S-PTC. Simulated curves were obtained using the parameters determined by the fitting of the $O_{1/S}O_1$ dose–response curves. (D) Induction of the gene circuits O_1-PTC and O_S-PTC. Simulated curves were obtained using the parameters determined by the fitting of the $O_{1/S}O_1T$ dose–response curves.

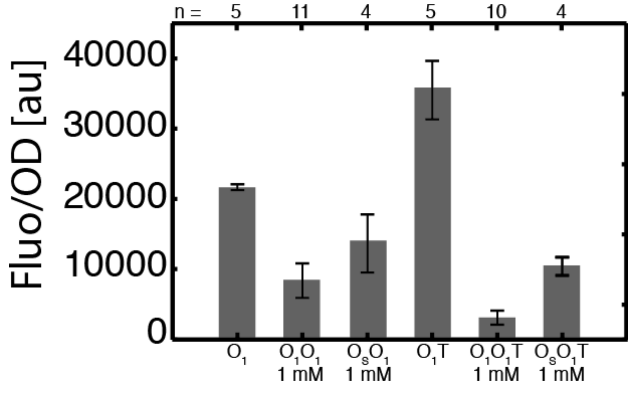

Figure 7. Effect of the TRANS sequence on GFP expression and response to IPTG induction. Gene circuits O_1, O_1T, $O_{1/S}O_1$, and $O_{1/S}O_1T$ are defined in Figure 5. Circuits $O_{1/S}O_1$ and $O_{1/S}O_1T$ were induced by 1 mM IPTG. Values are shown as average ± SD. The number of samples (n) is reported along the upper x-axis.

O_1 operator sites had to be increased by a factor of ~5. Thus, to prove that the TRANS sequence had such a strong effect on the affinity of the LacI operator site, we tested experimentally this hypothesis using a gel-shift assay. To this aim, pure LacI was used, along with plasmids containing the gene circuits O_1 and O_1T linearized by restriction digestion with the XbaI enzyme. The binding reactions were carried out with a constant concentration of DNA (3 nM), while the concentration of LacI was varied between 0 and 90 nM (see Methods section for more details). In the presence of O_1 DNA a modest shift in electrophoretic mobility was observed at LacI concentrations between 6 and 18 nM (Figure 8A, lanes 2–4). Conversely, in the presence of O_1T DNA, the same LacI concentrations caused a pronounced shift in electrophoretic mobility (Figure 8A, lanes 9–11). When a large excess (e.g., 60 nM) of tetrameric LacI was used, the electrophoretic mobility of both O_1 DNA and O_1T DNA was affected to a similar degree (Figure 8A, lanes 7 and 14, respectively). Figure 8B shows the relative electrophoretic mobilites (Rf) of both DNAs as a

dx.doi.org/10.1021/sb200021s | ACS Synth. Biol. 2012, 1, 163–171

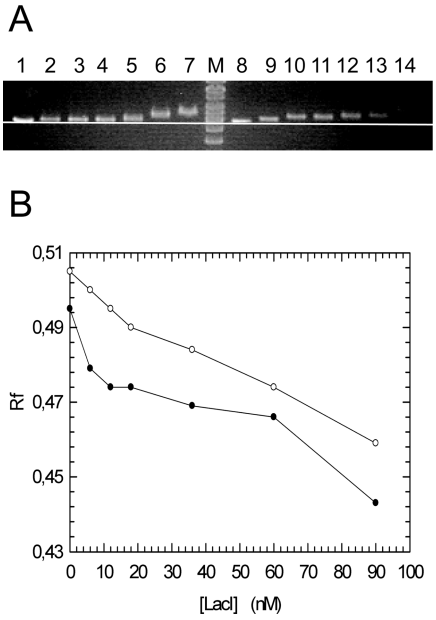

Figure 8. Gel-shift experiments. (A) Agarose gel electrophoresis of gel shift assay mixtures containing 3 nM linear DNA (pSB1A2/P2547-O_1-GFP and pSB1A2/P2547-O_1-TRANS-GFP, lanes 1−7 and 8−14, respectively) and 0, 6, 12, 18, 36, 60, or 90 nM LacI (lanes 1−7 and 8−14, respectively). Lane "M" was loaded with molecular mass markers (GeneRuler 1 kbp Ladder, Fermentas), and the horizontal white line was drawn just below the 3 kbp marker. The concentration of LacI is expressed in tetrameric form. (B) Relative electrophoretic mobility (Rf) of pSB1A2/P2547-O_1-GFP (O_1) (empty circles) and pSB1A2/P2547-O_1-TRANS-GFP (O_1T) (filled circles) DNA as a function of LacI concentration. The data were calculated from the gel reported in panel A.

function of LacI concentration. The Rf of O_1 DNA decreases from 0.505 in the absence of LacI to 0.495 in the presence of 60 nM LacI, and under the same conditions the Rf of O_1T DNA decreases from 0.495 to 0.433. Thus, at saturating LacI concentrations (60 nM of LacI corresponds to a 20-fold excess of LacI over DNA) Rf decreases by 10% for both DNAs. This effect is likely due to both specific and non-specific binding of lactose repressor to DNA. When lower concentrations of LacI were used, the slope of the Rf as a function of LacI concentration is clearly different between O_1 and O_1T DNA. While 36 nM LacI was necessary to shift the Rf of O_1 DNA by 4% (from 0.505 to 0.484), 12 nM LacI did suffice to trigger the same effect in the presence of O_1T DNA (from 0.495 to 0.474). Accordingly, we consider that the affinity of LacI toward O_1T DNA is about 3-fold higher when compared with O_1 DNA. The increase in affinity estimated by the gel-shift assay is remarkably close to the value predicted by mathematical modeling. When interpreting the difference between the increase in affinity predicted by the mathematical modeling (∼5) and the increase in affinity measured by the gel-shift experiment (∼3), it is important to keep in mind that one value is calculated through a fitting procedure of experimental data of fluorescence in a cell population, while the other value is the result of an *in vitro* experiment. In this perspective, the concurrence of the two approaches strongly support the hypothesis that the failure of the bottom-up approach in predicting the behavior of the O1/S-PTC gene circuits was due to the effect of the TRANS sequence on the affinity of the lactose operator sites.

The design of a circuit by a pure bottom-up approach requires that the presence of a module does not affect the behavior of the other modules. This is not true for the gene circuits analyzed in this study, since the presence of the TRANS sequence had a dramatic effect on the affinity of the lactose repressor for the operator sequences. In order to predict the behavior of the $O_{1/S}$-PTC circuits by mathematical modeling, it was necessary to estimate the parameters of the building blocks in circuits where two modules (TRANS sequence and operator sequence) were assembled together. These results are in agreement with previous observations that parts may behave differently when placed in different gene networks.[20,21] When the gene circuits $O_{1/S}O_1$T were used to characterize the elementary blocks, the characteristics of the $O_{1/S}$-PTC gene circuits could be quantitatively predicted by mathematical modeling. This result partially restores the validity of a bottom-up design strategy. However, for this approach to be useful it is necessary to establish a set of rules to be used for the characterization of the parts, and it is currently not clear if such a set can actually be established. If this does not exclude a rigorous description and characterization of part behavior and functionality, it puts doubts on the effective possibility of a pure bottom-up approach, where parts are once characterized and then used for the *a priori* prediction of the desired network outcome.

Part characterization must also consider that gene circuits may behave differently in different metabolic stages. This is certainly not entirely new,[22−24] but it needs to be overtly pointed out. Only by considering the whole network behavior is it possible to fully characterize a system and compare different cell populations. In this respect, we also showed here that the functionality of our device changed depending on cell growth phase and that only when cell populations reached OD from 0.7 to 0.9 were results consistent and reproducible.

In summary, our results call the attention of synthetic biologists to the importance of giving the proper consideration to functional modularity of biological parts and the need for a case-to-case characterization of their function, raising concern about the use of a overconfident bottom-up approach in synthetic biology and supporting the idea that emerging properties are a rule in nature that we must consider in the application of engineering principles to biology.

METHODS

CIS and TRANS Sequence Design. CIS and TRANS are 50-base-pair-long complementary sequences designed using a homemade software (for details see: http://2009.igem.org/Team:Bologna/Software) aimed at analyzing RNA sequences in order to avoid secondary structure formation as the result of intramolecular annealing and minimal unwanted interactions with genomic mRNA and to have minimal probability of partial/shifted hybridization with complementary strands. These specifications were desired for the proper engineering of the TRANS and CIS complementary sequences. Since the CIS sequence was planned to be placed upstream of a gene sequence of interest, to be regulated by the silencing mechanism, the TRANS was designed to contain a 4-base-pair tail complementary to the first 4 bases of the RBS placed in the CIS element, in order to maximize translation repression. This design was aimed to generate a CIS and TRANS that can be considered universal and useful for a modular silencing of the expression of any gene of interest cloned downstream of the CIS. After having generated a 50-bp-long sequence, the

software was used to check that the sequences did not contain (i) more than 5 adjacent repeats of the same nucleotide (to avoid transcription errors), (ii) restriction sites, and (iii) RBS sequences.

Plasmid Construction. All of the biological parts were taken from the Registry of Standard Biological parts except for the CIS and TRANS sequences that were synthesized (Invitrogen) in the BioBrick standard format. The *PT-Controller* circuit was cloned in a high copy number plasmid (pSB1A2) containing ampicillin resistance and a pUC19-derived pMB1 replication origin. The *Repressor* gene circuit was cloned in a medium copy number plasmid (pSB3K3) containing kanamycin resistance and a pMR101-derived p15A replication origin.

Two lactose operator sequences were used: O_1, aattgtgagcg-gataacaatt and O_S, aattgtgagcgctcacaatt.[25,26] The CIS sequence containing the RBS (Table 1) was cloned upstream of a GFP gene (BBa_J04631) with a LVA degradation tag. The CIS-GFP sequence was then placed downstream of the P1429 promoter (BBa_J23118) in the high copy number plasmid. The TRANS sequence (Table 1) was placed downstream of the O_1 Lac operator sequence, and the O_1-TRANS was then placed downstream of the P2547 promoter (BBa_J23100). P1429-CIS-GFP and P2447-O_1-TRANS, here named *Reporter* and *Silencer*, respectively, were then cloned on the same high copy number plasmid to form the *PT-Controller* plasmid. The *Repressor* plasmids with O_1 and O_S have a LacI-coding sequence with LVA degradation tag (BBa_C0012) placed downstream of the P1429-$O_{1/S}$ regulated promoter in the medium copy number plasmid. The same ribosome binding site (RBS) sequence (BBa_B0034) was cloned upstream of all of the protein coding sequences. A double transcriptional terminator T (BBa_B0015) was placed downstream of each transcriptional unit. Moreover, a double terminator is present at both sides of the plasmid multiple cloning site in order to prevent random transcriptions. As control constructs, we also built (i) Plasmid with P1429-CIS-GFP alone; (ii) a *PT-Controller* plasmid lacking the TRANS sequence; and (iii) a P2547-O_1-TRANS-GFP device.

Fluorescence Measurements. *E. coli* CSH126 cells were grown at 37 °C in Erlenmeyer flasks in 5 mL of M9 minimal medium supplemented with casamino acids, thiamine hydrochloride, and the proper antibiotics, with glucose as the main carbon source (Sigma). Time-course measurements were performed, where cells were grown up to 13 h and sampling done every 60 min for all of the different cell cultures. A sample of 200 μL was transferred into a multiwell plate from each cell culture. For each well both fluorescence (Fluo: Ex 501/Em 511 nm) and optical density (OD: 600 nm) were measured in an InfiniteM200 multiplate reader (Tecan) to follow bacterial cell and fluorescence growth over time. Fluorescence was divided by the OD value, in order to define a normalized value. A preliminary study confirmed the linear correlation between the fluorescence and the OD in the selected OD range, which justifies the fluorescence normalization performed.

Purification of LacI Repressor. A single colony of *Escherichia coli* TOP10/pBAD-*lacI* was dispersed in 5 mL of LB medium containing ampicillin (100 μg/mL). After overnight incubation at 37 °C, the culture was diluted (1:100) in fresh LB medium and grown at 30 °C for 6 h, and arabinose (13 mM) was then added to induce *lacI*. After overexpression of LacI for 3 h at 30 °C under shaking conditions (180 rpm), bacterial cultures were harvested by centrifugation. Cells pellets (from 900 mL cultures) were resuspended in 35 mL of 50 mM Tris-HCl pH 7.4, 5 mM EDTA, 1 mM DTT, 1 mM PMSF then sonicated on ice (Misonix-3000 sonifier) at 6 W level (7 cycles).

The protein extract was centrifuged at 10,000*g* for 20 min at 4 °C, and the supernatant was recovered. Soluble proteins were precipitated with ammonium sulfate (50% saturation). The protein pellet was resuspended in 30 mL of 50 mM Tris-HCl pH 8, 50 mM KCl, 1 mM EDTA, and 1 mM DTT and then dialyzed against the same buffer (1 L) for three times.

The dialyzed sample was loaded onto a 1.6 × 70 Superdex 200 column (GE Healthcare Life Sciences) equilibrated with Tris-HCl pH 8, 50 mM KCl, 1 mM EDTA, 1 mM DTT. Gel filtration was performed at 0.6 mL/min. The eluted fractions (0.9 mL) were analyzed by SDS-PAGE, and those enriched in LacI were then pooled. Final purification was achieved by anion exchange chromatography, using a ResourceQ column (1 mL, GE Healthcare Life Sciences), equilibrated with Tris-HCl pH 8, 1 mM EDTA, 1 mM DTT. The elution was performed with a 50−400 mM KCl linear gradient. Eluted fractions (0.2 mL) were loaded on SDS-PAGE (12.5%). The major LacI peak eluted approximately at 290−300 mM KCl. The fractions containing pure LacI were pooled, and the protein concentration was determined by the Bradford assay.

DNA Preparation. *E. coli* CSH126 cells containing the constructs P2547-O_1-GFP and P2547-O_1-TRANS-GFP in the high-copy number plasmid (pSB1A2) were grown overnight at 37 °C, under shaking (180 rpm), in LB medium containing ampicillin (100 μg/mL). Bacterial cells were harvested by centrifugation, and the plasmid DNA was purified with Qiagen Midi Prep columns, according to the manufacturer's instructions. Twenty micrograms of each plasmid was digested with *Xba*I (New England Biolabs, NEB) in a 200 μL reaction containing NEB Buffer 3 and BSA, at 37 °C for 2 h. The linearized DNA was visualized in agarose gels, extracted from the gel using the Freeze 'N Squeeze extraction columns (Bio-Rad), and then concentrated (Montage PCR, Millipore). Purified fragments were used in the gel shift assay with the purified LacI repressor.

Gel Shift Assay. Reaction mixtures (20 μL) contained a constant amount of DNA (3 nM) and increasing concentrations of purified LacI repressor in binding buffer (50 mM Tris-HCl pH 8, 100 mM KCl, 1 mM EDTA): 6, 12, 18, 36, 60, and 90 nM (in tetrameric form). A negative control reaction without LacI was also prepared. The assay mixtures were incubated at 20 °C for 25 min, 4 μL of 6X Loading dye (Fermentas) was then added, and the reactions were loaded on a TAE agarose gel (0.8%). Bands were detected with ethidium bromide staining, using a Gel-Doc system (Bio-Rad). GeneRuler 1 kbp Ladder (Fermentas) was used as DNA molecular mass marker.

Statistical Analysis. Values are reported as mean ± SD. One-way ANOVA and the Bonferroni posthoc test for pairwise comparisons were used for detecting differences in normalized fluorescence between multiple groups, for which normal distributions were found (Jarque-Bera test). A significance level of 95% ($p < 0.05$) was used for all of the statistical analyses. MATLAB package (2007a, The MathWorks, Natick, MA) was used for the statistical tests.

Mathematical Model and Parameter Definition. The rate of change of GFP molecules (G) was modeled by a first-order differential equation:

$$\frac{dG}{dt} = \alpha_G M_G - \lambda_G G \quad (1)$$

where M_G is the number of mRNA molecules available for transcription, α_G is the number of protein produced per mRNA molecule in the time unit, and λ_G is the degradation rate. In the complete gene circuit, the number of mRNA molecules available to transcription depends not only on transcription and degradation rates but also on the sequestration of mRNA molecules due to CIS−TRANS coupling.

$$\frac{dM_G}{dt} = \alpha_G^M D_R^0 - \lambda_G^M M_G - k^{HYB} M_G M_T. \quad (2)$$

In eq 2, we assumed that the pairing of mRNA molecules is an irreversible process. The dynamics of the mRNA molecules of the TRANS circuit was modeled with an analogous equation:

$$\frac{dM_T}{dt} = \alpha_T^M D_T^F - \lambda_T^M M_T - k^{HYB} M_G M_T \quad (3)$$

However, while in eq 2 the number of encoding sequences available to transcription is constant to D_G^0, the binding of LacI molecules to the operator sequence O_1 on the *Silencer* modulates the number of TRANS sequences available for transcription. The number of free promoter was described as

$$D_T^F = D_R^0 - D_T^L - D_T^I \quad (4)$$

where D_T^0 is the total number of plasmids, D_T^L is the number of promoters bound to LacI molecules, and D_T^I is the number of promoters bound to LacI-IPTG complexes. The binding of LacI molecules to operator sites was described by

$$\frac{dD_T^L}{dt} = \frac{1}{\tau_T^{DL}}\left[\frac{L^F D_T^F}{K_T^{DL}} - D_T^L\right] \quad (5)$$

$$\frac{dD_T^I}{dt} = \frac{1}{\tau_T^{DI}}\left[\frac{L^I D_T^F}{K_T^{DI}} - D_T^I\right] \quad (6)$$

Equations analogous to eqs 3−6 were used to describe the synthesis of mRNA molecules of LacI:

$$\frac{dM_L}{dt} = \alpha_L^M D_L^F - \lambda_L^M M_L \quad (7)$$

$$D_L^F = D_L^0 - D_L^L - D_L^I \quad (8)$$

$$\frac{dD_L^L}{dt} = \frac{1}{\tau_L^{DL}}\left[\frac{L^F D_L^F}{K_L^{DL}} - D_L^L\right] \quad (9)$$

$$\frac{dD_L^I}{dt} = \frac{1}{\tau_L^{DI}}\left[\frac{L^I D_L^F}{K_L^{DI}} - D_L^I\right] \quad (10)$$

Finally, the number of free LacI molecules, L^F, and LacI molecules bound to IPTG, L^I, were modeled as

$$\frac{dL^F}{dt} = \alpha_L M_L - \lambda_L L^F - \frac{1}{\tau^{LI}}\left[L^F\left(\frac{I}{K^{LI}}\right)^{n^{LI}} - L^I\right] - \frac{dD_L^L}{dt} - \frac{dD_T^L}{dt} \quad (11)$$

$$\frac{dL^I}{dt} = +\frac{1}{\tau^{LI}}\left[L^F\left(\frac{I}{K^{LI}}\right)^{n^{LI}} - L^I\right] - \lambda_L L^I - \frac{dD_L^I}{dt} - \frac{dD_T^I}{dt} \quad (12)$$

The list of state variables and parameters of the model are summarized in Supporting Tables 1 and 2.

All of the parameters of the model were taken from ref 3 except for the equilibrium binding constant of LacI-IPTG complexes to the operator sites, $K_{1/S}^I$; the LacI-IPTG binding constant, K^{LI}; and the forward binding constant for the CIS−TRANS annealing reaction, k^{HYB}. In ref 3 the parameters $K_{1/S}^I$ and K^{LI} were determined by fitting the experimental dose response curves of gene circuits analogous to $O_S O_1$ and $O_1 O_1$. The fitting was repeated using the dose−response curves of $O_S O_1$ and $O_1 O_1$ obtained in the specific experimental conditions adopted here. The model defined by this procedure provided an accurate description of the experimental data of the $O_{1/S} O_1$ circuits (Figure 5A), which was the basis for testing the modularity of the final network. The binding constant for the CIS−TRANS annealing was defined by simulating a system without the *Repressor* circuit, in the presence or absence of the CIS−TRANS annealing reaction. The system was first simulated with the annealing reaction turned off and then in the presence of the annealing reaction, and the decrease in the GFP level was calculated. The value of k^{HYB} was the one that minimized the distance between this simulated GFP reduction and the fluorescence reduction in cells transformed with the *PT-Controller* without/with the TRANS sequence (circuits d and e in Figure 2). In order to reproduce the dose−response curves of the $O_{S/1} O_1$T gene circuits, the binding affinities of the lactose repressor to the operator site on the *Silencer* plasmid were increased by a constant ratio, which was determined by minimizing the distance from the experimental data.

■ ASSOCIATED CONTENT

Supporting Information

List of state-variables and parameters of the mathematical model. This material is available free of charge via the Internet at http://pubs.acs.org.

■ AUTHOR INFORMATION

Corresponding Author

*Tel: +39 0547 339243. E-mail: francesca.ceroni2@unibo.it.

Author Contributions

[+]These authors contributed equally to this work.

Author Contributions

F.C. built the genetic constructs used in this work and planned and performed all of the experimental measurements. A.F. and A.H. produced the recombinant LacI and implemented the gel-shift assay. S.F. developed the mathematical model and performed the fitting procedure and parameter identification. E.G. advised on wet-lab procedures and planned and occasionally performed the experiments. All authors wrote, read. and approved the final manuscript.

Notes

The authors declare no competing financial interest.

■ ACKNOWLEDGMENTS

Elisa Passini, Marilisa Cortesi, and Andrea Samorè participated in some of the experiments presented in this work. We want to thank Dr Alice Pasini for fruitful discussion about our

experiments. We also want to remember here the late Prof. Silvio Cavalcanti, a friend, a co-founder of the Laboratory of Cellular and Molecular Engineering, and an experienced scientist in the fields of numerical modeling and Synthetic Biology. His unexpected passing deprived us of a significant contribution to this work, as it was originally planned.

REFERENCES

(1) Beisel, C. L., Bayer, T. S., Hoff, K. G., and Smolke, C. D. (2008) *Mol. Syst. Biol. 4*, 224.
(2) Ellis, T., Wang, X., and Collins, J. J. (2009) *Nat. Biotechnol. 27*, 465−71.
(3) Ceroni, F., Furini, S., Giordano, E., and Cavalcanti, S. (2010) *J. Biol. Eng. 4*, 14.
(4) Elowitz, M. B., and Leibler, S. (2000) *Nature 403*, 335−8.
(5) Gardner, T. S., Cantor, C. R., and Collins, J. J. (2000) *Nature 403*, 339−42.
(6) Cox, R. S., Dunlop, M. J., and Elowitz, M. B. (2010) *J. Biol. Eng. 4*, 10.
(7) Madar, D., Dekel, E., Bren, A., and Alon, U. (2011) *BMC Syst. Biol. 5*, 111.
(8) Amit, R., Garcia, H. G., Phillips, R., and Fraser, S. E. (2011) *Cell 146*, 105−18.
(9) Haynes, K. A., and Silver, P. A. (2011) *J. Biol. Chem. 286*, 27176−82.
(10) Isaacs, F. J., Dwyer, D. J., and Collins, J. J. (2006) *Nat. Biotechnol. 24*, 545−54.
(11) Babiskin, A. H., and Smolke, C. D. (2011) *Mol. Syst. Biol. 7*, 471.
(12) Malphettes, L., and Fussenegger, M. (2006) *Metab. Eng. 8*, 672−83.
(13) Isaacs, F. J., Dwyer, D. J., Ding, C., Pervouchine, D. D., Cantor, C. R., and Collins, J. J. (2004) *Nat. Biotechnol. 22*, 841−7.
(14) Win, M. N., and Smolke, C. D. (2007) *Proc. Natl. Acad. Sci. U.S.A. 104*, 14283−8.
(15) Kelly, J. R., Rubin, A. J., Davis, J. H., Ajo-Franklin, C. M., Cumbers, J., Czar, M. J., de Mora, K., Glieberman, A. L., Monie, D. D., and Endy, D. (2009) *J. Biol. Eng. 3*, 4.
(16) Canton, B., Labno, A., and Endy, D. (2008) *Nat. Biotechnol. 26*, 787−93.
(17) Oehler, S., Amouyal, M., Kolkhof, P., von Wilcken-Bergmann, B., and Muller-Hill, B. (1994) *EMBO J. 13*, 3348−55.
(18) Berg, L., Lale, R., Bakke, I., Burroughs, N., and Valla, S. (2009) *Microb. Biotechnol. 2*, 379−89.
(19) Park, Y. S., Seo, S. W., Hwang, S., Chu, H. S., Ahn, J. H., Kim, T. W., Kim, D. M., and Jung, G. Y. (2007) *Biochem. Biophys. Res. Commun. 356*, 136−41.
(20) Salis, H. M., Mirsky, E. A., and Voigt, C. A. (2009) *Nat. Biotechnol. 27*, 946−50.
(21) Voigt, C. A. (2006) *Curr. Opin. Biotechnol. 17*, 548−57.
(22) Hugouvieux-Cotte-Pattat, N., Kohler, T., Rekik, M., and Harayama, S. (1990) *J. Bacteriol. 172*, 6651−60.
(23) Ishihama, A. (1997) *Curr. Opin. Genet. Dev. 7*, 582−8.
(24) Ishihama, A. (1999) *Genes Cells 4*, 135−43.
(25) Gilbert, W., and Maxam, A. (1973) *Proc. Natl. Acad. Sci. U.S.A. 70*, 3581−4.
(26) Sadler, J. R., Sasmor, H., and Betz, J. L. (1983) *Proc. Natl. Acad. Sci. U.S.A. 80*, 6785−9.